The p recombination layer in tunnel junctions for micromorph tandem solar cells*

Yao Wen-Jie(姚文杰), Zeng Xiang-Bo(曾湘波)†, Peng Wen-Bo(彭文博), Liu Shi-Yong(刘石勇), Xie Xiao-Bing(谢小兵), Wang Chao(王 超), and Liao Xian-Bo(廖显伯)

Key Laboratory of Semiconductor Materials Science, Institute of Semiconductors, Chinese Academy of Sciences, Beijing 100083, *China*

(Received 7 January 2011; revised manuscript received 10 March 2011)

A new tunnel recombination junction is fabricated for n–i–p type micromorph tandem solar cells. We insert a thin heavily doped hydrogenated amorphous silicon (a-Si:H) p^+ recombination layer between the n a-Si:H and the p hydrogenated nanocrystalline silicon (nc-Si:H) layers to improve the performance of the n–i–p tandem solar cells. The effects of the boron doping gas ratio and the deposition time of the p-a-Si:H recombination layer on the tunnel recombination junctions have been investigated. The current-voltage characteristic of the tunnel recombination junction shows a nearly ohmic characteristic, and the resistance of the tunnel recombination junction can be as low as 1.5 $\Omega\cdot$cm^2 by using the optimized p-a-Si:H recombination layer. We obtain tandem solar cells with open circuit voltage $V_{\rm oc} = 1.4$ V, which is nearly the sum of the $V_{\rm oc}$s of the two corresponding single cells, indicating no $V_{\rm oc}$ losses at the tunnel recombination junction.

Keywords: p recombination layer, tunnel recombination junction, micromorph tandem solar cells

PACS: 84.60.Jt, 81.15.Gh, 73.40.Lq, 73.40.–c **DOI:** 10.1088/1674-1056/20/7/078402

1. Introduction

Micromorph tandem solar cells have attracted great interest for their potential to achieve high conversion efficiencies at relatively low cost.[1,2] The micromorph tandem cells make better use of the sun spectrum compared to a-Si:H/a-Si:H stacked cells.[3] The micromorph tandem cells basically consist of two n–i–p devices in series. In the cells, the short wavelength light is absorbed in the top a-Si:H cell and the long wavelength light is absorbed in the bottom μc-Si:H cell.[4] The adjacent n and p layers of the two component cells form a potential barrier, usually called the tunnel recombination junction (TRJ), which might result in a carrier accumulation. The electrons generated in the top cell and the holes generated in the bottom cell can recombine by tunneling into defect states at the n/p interface, while the holes generated in the top cell and the electrons generated in the bottom cell will go through the load and form a complete current loop. The quality of the TRJ is crucial to obtain high-efficiency tandem cells. If the photogenerated carriers were built up at the junction, the piled charges would corrupt the electric field inside the cell and even generate photovoltage in the reverse direction. As a result, the tandem cells will have a low fill factor (FF) and a low open circuit voltage ($V_{\rm oc}$). Thus some concerns of the junction are the efficiency of the carrier recombination, the reverse photovoltage and the transparency. A good tunnel junction should show ohmic behaviour to allow very high recombination rates.

Three approaches have been developed for making improved TRJs. The first one inserts metal oxides such as TiO_x[5] and NbO_x[6] into the a-Si:H n/p junction acting as the recombination layers. The metal oxides with high optical transparency can provide enough recombination centres. However, this method is not compatible with the chemical vapor deposition (CVD) processing of the monolithic tandem cells. The second approach is to improve the n-μc-Si:H/p-μc-Si:H tunnel junction by using the oxidation treatments,[7,8] such as CO_2 plasma oxidation and air break at the n/p interface, which enhance the recombination. As the method of oxidation treatment can

*Project supported by the National Basic Research Program of China (Grant No. 2006CB202604), the Knowledge Innovation Program of Chinese Academy of Sciences (Grant No. 1KGCX2-YW-383-1), and the National High Technology Research and Development Program of China (Grant No. SQ2010AA0521758001).

†Corresponding author. E-mail: xbzeng@semi.ac.cn

© 2011 Chinese Physical Society and IOP Publishing Ltd

not be controlled easily, the oxidation treatment is replaced by using an intrinsic microcrystalline silicon interface layer.[9] The third approach is to improve the n-a-Si:H/p-SiC:H or n-μc-Si:H/p-SiC:H tunnel junction by inserting a thin p-a-Si:H layer. The thin p-a-Si:H layer, which has a higher conductivity than the p-a-SiC:H, can improve the tunnel junction by providing a larger supply of holes for recombine with the electrons from the n layer.[10,11]

The purpose of making tunnel junctions is to improve the carrier recombination at the interface of the n and the p layers. All the approaches mentioned above focus on this purpose. Both the p-SiC:H and the p-nc-Si:H layers are wide gap materials, the p-nc-Si:H layer has a higher conductivity (10^{-1} S/cm) compared to the p-SiC:H layer (10^{-6} S/cm), hence the hole injection from the μc-Si:H bottom cell can be improved greatly by using a p-nc-Si:H layer. Nevertheless, the wide gap is not favorable for recombination if a p-nc-Si:H layer is used as the window layer at the bottom cell. In this paper, a p-a-Si:H layer with a narrower band gap was inserted at the interface of the n-a-Si:H/p-nc-Si:H connect junction to make the recombination process more effective.

2. Experiment

The TRJs were made on stainless steel (SS) substrates and the structure was SS /p-nc-Si:H/p^+-a-Si:H /n-a-Si:H/indium tin oxide (SS/p/p^+/n/ITO). All layers were deposited in a three-chamber capacitive coupled radio-frequency (RF of 13.56 MHz) plasma-enhanced chemical vapor deposition (PECVD) system. The reaction gases were H_2, SiH_4 (100%) and B_2H_6 (1%, diluted by H_2). Deposition parameters for each layer (except the p^+ layer) are listed in Table 1. Boron-doped hydrogenated silicon p^+ films were deposited with a fixed hydrogen dilution ratio (SiH_4/H_2) 1/10. Firstly, the tunnel junctions with and without the p^+ layer were deposited to assess the role of the inserted p^+ layer. Then two series of TRJs were made to investigate the effect of the p^+ layer on the TRJs: one with the doping gas ratio of the p^+ layer changed; the other with the thickness of the p^+ layer changed by varying the depositing time.

Table 1. Deposition parameters of each layer in TRJs.

	Substrate temperature/°C	Pressure/Pa	Power/mW·cm^{-2}	Reaction gas
p-nc-Si:H	150	650	1000	SiH_4:H_2:B_2H_6(1%)=1:100:2
n-a-Si:H	150	200	100	SiH_4:H_2:PH_3(1%)=6:60:10

Micromorph tandem solar cells were fabricated to evaluate the performance of the optimum n-a-Si:H/p-a-Si:H/p-nc-Si:H tunnel junction. The micromorph tandem cells had the structure of [SS/Ag/AZO/n-μc-Si:H layer/i-μc-Si:H layer/p-nc-Si:H layer/p-a-Si:H recombination layer/n-a-Si:H layer/i-a-Si:H layer/p-nc-Si:H layer/ITO]. The area of the ITO dot was 0.07 cm^2. The cell performance was characterized by photocurrent density–voltage measurement with a xeon solar simulator (100 mW/cm^2, calibrated by a standard silicon solar cell) and a Keithley 2400 source meter at room temperature.

3. Results and discussion

Figure 1 shows the current density (J) versus the voltage (V) (J–V) curves of the two tunnel junctions with and without the p-a-Si:H insertion layer. The doping ratio (B_2H_6/SiH_4) and the deposited time of the p-a-Si:H insertion layer were 0.67% and 10 s, respectively. The J–V curve shows that the TRJ with the p-a-Si:H insertion layer has a higher conductivity compared to its counterpart. The p layer in our micromorph cells is typically nc-Si:H, which has a high electrical conductivity (∼0.6 S/cm), a low activation energy (0.06 eV) and a wide optical band gap (2.0 eV).[12] The high conductivity can reduce the series resistance, the low activation energy can increase the built-in potential in the intrinsic absorber layer and the wide optical band gap can reduce the optical absorption. Due to the high electrical conductivity, the p-nc-Si:H layer in the tunnel junction can provide enough holes for recombination with the electrons from the n layer. However, the wide band gap of the p-nc-Si:H layer does not favor the recombination in the middle of the tunnel junction. In addition, the activation energy of the p-nc-Si:H layer is low and the Fermi levels locate near the valence band edge far from the mid-gap, which do not facilitate recombination either. An inserted narrow band gap p-a-Si:H layer provides a narrow region where carriers can recombination effectively. In addition, the Fermi level

closer to the mid-gap in the p-a-Si:H layer improves the recombination by providing approximately equal supplies of holes and electrons. It can be seen from Fig. 1 that the inserted p-a-Si:H layer improves the recombination.

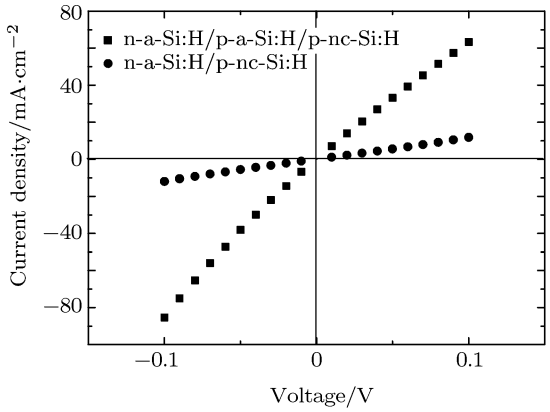


Fig. 1. The J–V curve of the tunnel junctions with and without p-a-Si:H insertion layer.

The J–V properties of the tunnel junction are sensitive to the doping ratio and the deposition time of the inserted p-a-Si:H layer. For the series with doping gas ratio changed, the deposition time of the p^+ layers was kept at 10 s. Plotting the J–V data as $R = V/J$ can more clearly identify the nonohmic behaviour. Figure 2 shows the voltage dependence of the resistance (V/J) of the series with doping gas ratios 0% (curve a), 0.67% (curve b), and 4% (curve c). It shows that the resistance of the tunnel junction is sensitive to the boron doping gas ratio of the p^+ layer. The sample with 0% boron doping gas ratio (intrinsic a-Si:H) insertion layer (curve a) exhibits a maximum resistance of about 24 $\Omega\cdot$cm^2 and an obvious nonohmic behaviour. This is because of the low defect density in the intrinsic a-Si:H material. Replacing the intrinsic a-Si:H insertion layer with a lightly doped ($B_2H_6/SiH_4 = 0.67\%$) a-Si:H layer lowers the maximum resistance by a factor of 12 and produces a nearly ohmic behaviour. This indicates that the doped ($B_2H_6/SiH_4 = 0.67\%$) a-Si:H layer enhances the recombination. It is reported that the defect density N_d in doped a-Si:H increased with the square root of the doping concentration C_g[13] ($N_\mathrm{d} = 3\times10^{19}C_\mathrm{g}^{1/2}$). For our 0.67% doping gas ratio (B_2H_6/SiH_4) samples, the corresponding doping concentration is 0.66% and the defect density is about 2.57×10^{18} cm^{-3}, while it is reported that the defect density of the intrinsic a-Si:H is less than 10^{16} cm^{-3}.[13] We propose that the doped ($B_2H_6/SiH_4 = 0.67\%$) a-Si:H insertion layer with a higher defect density provides enough defects for recombination, thus improves the properties of the TRJ.

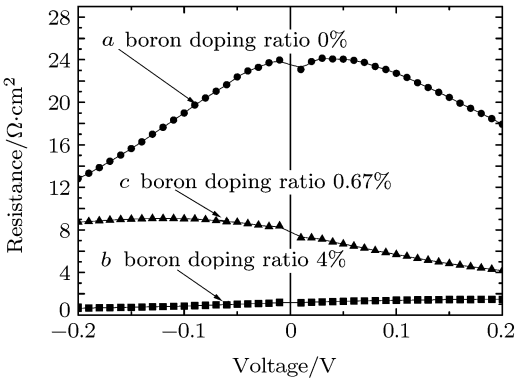


Fig. 2. Voltage dependence of resistance (V/J) of TRJs with various boron doped p^+ inserted layers.

It should be noted that the boron doping gas ratio of the inserted a-Si:H layer can not be very high. When the boron doping gas ratio of the p-a-Si:H insertion layer increases to 4%, the resistance of the tunnel junction rises and the J–V data shows nonohmic behaviour again (curve c). At these high doping levels, the material is more properly described as an alloy with a large decrease in the conductivity.[13] Consequently, the optimum boron doping gas ratio for the p-a-Si:H insertion layer is 0.67% for our system.

The J–V behaviour of the tunnel junction could be affected by the thickness of the inserted recombination layer.[9,11] We fabricated another series of TRJs with different p^+ deposition time. Figure 3 shows the voltage dependence of the resistance of the series with the p^+ layers deposited in 5 s, 10 s and 15 s. All boron doping gas ratio of the p^+ layers was kept at 0.67%. The sample deposited in 5 s shows nonohmic behaviour and the maximum resistance increases to 5.5 $\Omega\cdot$cm^2. This is ascribed to that the p^+ layer deposited in 5 s is too thin to provide enough recombination centres for the recombination. Increasing the deposition time to 10 s, the TRJ shows ohmic behaviour and a smaller resistance (as low as 1.5 $\Omega\cdot$cm^2). Increasing the deposition time to 15 s, the TRJ shows nonohmic behaviour again and the maximum resistance is about 8 $\Omega\cdot$cm^2. This can be explained by that the p-a-Si:H insertion layer deposited in 15 s is too thick, which results in the resistance increase. Figure 4 shows the quantum efficiencies (QEs) of these three samples with p-a-Si:H insertion layers deposited in 5 s, 10 s and 15 s. The lowest QE is obtained from the sample with the p-a-Si:H insertion layer deposited for 10 s, which reveals that most carriers are recombined in the TRJ. The thicker p-a-Si:H layers (15 s) impede the hole transport, as a result less holes are

provided for recombination and the QE goes up. Accordingly, it suggests that the p-a-Si:H insertion layer deposited in 10 s provides the greatest recombination.

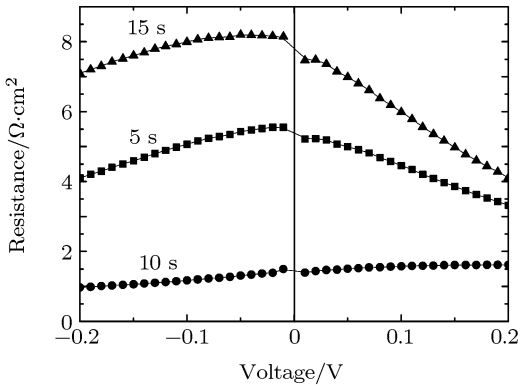


Fig. 3. Voltage dependence of resistance (V/J) of TRJs with various P^+ layer deposition time.

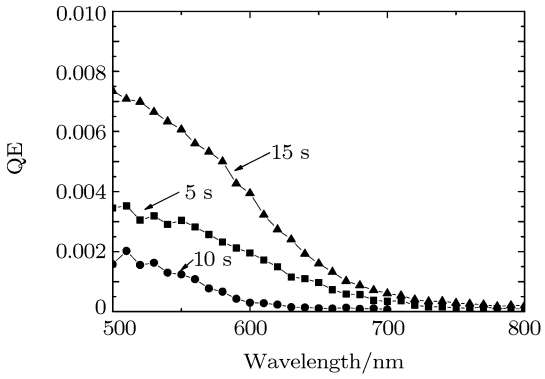


Fig. 4. Quantum efficiency at 0 V for the same TRJs in Fig. 3.

The E_a indicates the carrier transport barrier crossing the tunnel junction.[11] Figure 5(a) shows the temperature dependence of the conductivity of the three samples with p-a-Si:H insertion layers deposited in 5 s, 10 s and 15 s. Figure 5(b) shows the E_a derived from Fig. 5(a). The E_a of the TRJ with insertion layer deposited in 10 s is almost half of that of the TRJs with insertion layers deposited in 5 s and 15 s. The conductivity of the TRJ with the p^+ layer deposited in 10 s is the highest among three samples.

To estimate the effect of the optimum n/p+/p TRJ on the performance, micromorph tandem solar cells were deposited. Figure 6 presents J–V characteristics of the tandem cells and that of the corresponding single junction cells under a xeon solar simulator irradiation. The conversion efficiency of the cells with the optimum n/p+/p TRJ is 10.27%. Table 2 is a list of short circuit current density (J_{sc}), V_{oc}, FF, and energy efficiency (E_{ff}). It is shown in Table 2 that the V_{oc} (1.4 V) of the tandem cells is the sum of the V_{oc}'s of the corresponding amorphous silicon single cell (0.89 V) and the microcrystalline silicon single cell (0.52 V). This indicates that the n/p+/p tunnel junction does provide enough recombination centres. If the tunnel junction did not provide enough recombination centres, charge would accumulate at the tunnel junction, which would result in a dipole layer with a reverse voltage bias and the tandem cells would have a lower V_{oc} than the sum of the V_{oc}'s of the two counterpart single junction cells.

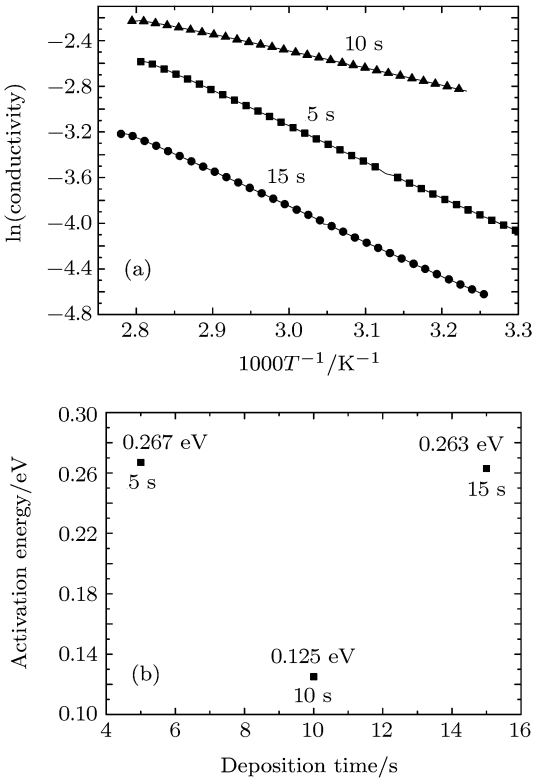


Fig. 5. (a) Temperature dependence of the conductivity of TRJs with different p^+ layer deposition time. (b) Activation energy of TRJS with different p^+ layer deposition time.

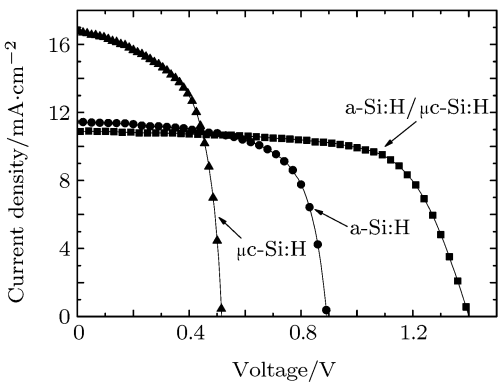


Fig. 6. Comparison of the current density–voltage characteristics of micromorph tandem solar cells with the single junction cells counterparts.

Table 2. Comparison of the performances of the tandem cells and the corresponding single junction cells.

Cell	V_{oc}/ V	J_{sc} /mA·cm^{-2}	FF	E_{ff}
a-Si:H single junction cell	0.89	11.4	0.66	6.72%
μc-Si:H single junction cell	0.52	16.7	0.63	5.14%
Micromorph tandem cell	1.40	10.8	0.68	10.27%

4. Conclusion

We have fabricated an n-a-Si:H/p-a-Si:H/p-nc-Si:H TRJ for n–i–p type micromorph tandem solar cells. The p-a-Si:H insertion layer with a narrower band gap and a Fermi level closer to the mid-gap improves the recombination. The J–V data of the optimum TRJ shows nearly ohmic behaviour and the resistance is as low as 1.5 Ω·cm^2. Using this TRJ in the n–i–p tandem solar cells, we have obtained V_{oc} of 1.4 V, which is nearly the sum of the corresponding subcells with V_{oc}'s of 0.89 V and 0.52 V respectively and exhibits no V_{oc} losses.

References

[1] Zhang X D, Zheng X X, Wang G H, Xu S Z, Yue Q, Lin Q, Wei C C, Sun J, Zhang D K, Xiong S Z, Geng X H and Zhao Y 2010 *Acta Phys. Sin.* **59** 8231 (in Chinese)

[2] Zhang X D, Zhang H, Wei C C, Sun J, Hou G F, Xiong S Z, Geng X H and Zhao Y 2010 *Chin. Phys.* B **19** 038101

[3] Keppner H, Meier J, Torres P, Fischer D and Shah A 1999 *Appl. Phys.* A **69** 169

[4] Chen Y S, Yang S E, Wang J H, Lu J X, Gao X Y and Gu J H 2010 *Chin. Phys.* B **19** 057205

[5] Sakai Y, Fukuyama K, Matsumura M, Nakato Y and Tsubomura H 1988 *J. Appl. Lett.* **64** 394

[6] Shen D, Schropp R, Chatham H, Hollingsworth R, Bhat P and Xi J 1990 *Appl. Phys. Lett.* **56** 1817

[7] Rath J K, Rubinelli F A and Schropp R E I 2000 *J. Non-Cryst. Solids* **266–269** 1129

[8] Li G J, Hou G F, Han X Y, Yuan Y J, Wei C C, Sun J, Zhao Y and Geng X H 2009 *Chin. Phys.* B **18** 1674

[9] Rubinelli F A, Rath J K and Schropp R E I 2001 *J. Appl. Phys.* **89** 4010

[10] Hegedus S S, Kampas F and Xi J P 1995 *Appl. Phys. Lett.* **67** 7

[11] Kwak J, Kwon S W and Lim K S 2006 *J. Non-Cryst. Solids* **352** 1847

[12] Liu S Y, Zeng X B, Peng W B, Xiao H B, Yao W J, Xie X B, Wang C and Wang Z G 2011 *J. Non-Cryst. Solids* **357** 121

[13] Street R A 1991 *Hydrogenated Amorphous Silicon* (New York: Cambridge University Press) pp. 135, 146